Surface Reactivity of the Au-Si-Ho Quasicrystalline 1/1 Approximant

Wilfried Bajoun Mbajoun, Yu-chin Huang, Girma Hailu Gebresenbut, Cesar Pay Gómez, V. Fournee, Julian Ledieu

Surface reactivity of the Au-Si-Ho quasicrystalline 1/1 approximant.

Wilfried Bajoun Mbajoun[1], Yu-Chin Huang[2], Girma Hailu Gebresenbut[2], Cesar Pay Gómez[2], Vincent Fournée[1], and Julian Ledieu[1]

[1]Institut Jean Lamour UMR 7198, Université de Lorraine-CNRS, Nancy, France
[2]Department of Chemistry-Ångström Laboratory, Uppsala University, SE-751 21 Uppsala, Sweden

Abstract

The oxidation of the (100) surface of Au-Si-Ho quasicrystalline approximant was studied using low-energy electron diffraction and X-ray photoelectron spectroscopy. The combination of these two techniques provides evidence for a Ho and Si surface segregation induced by O_2 adsorption, resulting in the loss of surface long-range order.

1 Introduction

The discovery of quasicrystals (QC) in 1982 by Dan Shechtman has generated a huge interest because of their unique structures and properties such as their low friction coefficients, low adhesion energies, good corrosion resistance and large catalytic activities [1–4]. Lacking translational periodicity in the 3-dimensional space, quasicrystals have an atomic arrangement that can be described by highly symmetric atomic clusters, building blocks assembled according to specific matching rules. For each quasicrystal usually corresponds one or more quasicrystalline approximants. The latter are periodic crystals that exhibit building blocks similar to those identified in the QC but arranged in a slightly different way such that they recover translational periodicity. The corrosion and oxidation resistance of QCs or complex metallic alloys to be more general have motivated the scientific community to carry out fundamental studies of their intrinsic surface properties upon oxygen adsorption under well-controlled experimental conditions. Studies of the oxidation behavior of quasicrystalline surfaces have been carried out mainly on Al-based systems such as the icosahedral Al-Pd-Mn and Al-Cu-Fe quasicrystals, the decagonal Al-Ni-Co quasicrystal as well as periodic tetragonal ω-Al_7Cu_2Fe phase [5–7], etc... In the majority of cases, oxygen adsorption at room temperature leads to Al surface segregation and the formation of an aluminum oxide layer showing no long-range order. The formation of periodically ordered oxide overlayers was only reported for i-Al-Pd-Mn and d-Al-Ni-Co upon oxygen adsorption and annealing at high temperatures [5, 6]. It can be mentioned that on intermetallics of lower structural complexity (Al_4Cu_9, Al_9Co_2), the successful growth of ultrathin alumina oxide (sixton-type) was achieved [8, 9].

The Au-Si-Ho quasicrystalline approximant has a structure close to MCd_6 (M=Ca, Yb) quasicrystal approximants that are prototypes of the Tsai-type quasicrystals [10–12]. It crystallizes in the

body-centered cubic structure and has a lattice parameter equal to 14.56 Å. This quasicrystalline approximant has been identified for its remarkable magnetic properties derived from its complex structure [13–15]. The Tsai-type clusters characteristic of these systems consist of concentric shells, the inner one being a disordered tetrahedron surrounded by a dodecahedron, an icosahedron, an icosidodecahedron, and finally a rhombic triacontahedron. The oxidation behavior of this family of quasicrystals has only been studied in the case of the i-Ag-In-Yb phase [16]. It was found that elements in the quasicrystal show oxidation behavior similar to that of the pure elements Ag, In, and Yb.

In this paper, we investigate the reactivity of Au-Si-Ho approximant surface prepared under ultra-high vacuum (UHV) conditions by adsorption of pure oxygen (O_2) at room temperature and at 573 K using low energy electron diffraction (LEED) and X-ray photoelectron spectroscopy (XPS).

2 Experimental methods

A single crystal was synthesized by self-flux technique as described in Ref. [13] and had a nominal chemical composition of $Au_{67.2}Si_{18.4}Ho_{14.4}$. The crystal was oriented by back-Laue diffraction and cut in order to expose a (100) surface. The surface was mechanically polished using diamond paste with decreasing grain size down to 0.25 µm leading to a mirror-like appearance. The single crystal was then inserted in the UHV system equipped with surface preparation tools, LEED and XPS. To obtain a clean surface, the surface preparation consisted of cycles of Ar+ sputtering (2 keV) followed by annealing at various temperatures. Surface crystalline order, cleanliness and overall chemical composition were studied by LEED and XPS using a non-monochromatized Mg K_α source. The clean and ordered surface was obtained after annealing the sample at least at 848 K. In situ oxidation was then performed by dosing the clean surface with pure O_2 (5N) at a pressure of 1.3×10^{-7} mbar and exposure ranging from 20 to 100 Langmuir (L).

3 Results and discussion

Figure 1 shows the LEED pattern recorded before and after surface oxidation under various conditions. From the LEED pattern obtained from the clean surface, we found a ratio of the surface lattice parameter (b/c) equal to 2, meaning that the surface undergoes a (2x1) reconstruction compared to the bulk lattice (further explanations on the surface reconstruction will be given in another communication). Figure 1(a) shows the evolution of the LEED pattern upon the initial stages of oxidation at room temperature. The background intensity increases with exposure to oxygen and there is a progressive loss of the LEED pattern. After adsorption of 100 L of O_2 several diffraction spots are still visible. After the adsorption of only 20 L at 573 K (Fig. 1(b)), the LEED pattern completely disappears, indicative of an amorphous surface induced by O_2 adsorption. This amorphization effect is slower at room temperature but faster at 573 K.

Angle-resolved X-ray photoelectron spectroscopy is used to measure the near-surface composition as a function of the surface sensitivity when the escape depth of the photoelectron is varied. The chemical composition expected from the bulk is $Au_{67.2}Si_{18.4}Ho_{14.4}$ in (at.%). Experimentally, the chemical composition in the near-surface region is obtained by quantifying the peak area of the XPS Au 4f, Ho 4d and Si 2s core levels after subtracting the Mg Kα satellites. The measured integrated intensity for each core level has been corrected by a normalization coefficient as described in Ref. [17]. Shirley background subtraction has been used for Au 4f, Ho 4d and Si 2s core level spectra.

The chemical composition of the clean surface obtained after sputtering and annealing the sample at 878 K is $Au_{68.2}Si_{14.6}Ho_{17.2}$ and $Au_{67.4}Si_{17.8}Ho_{14.8}$ for photoelectrons take-off angle equal to 0° and

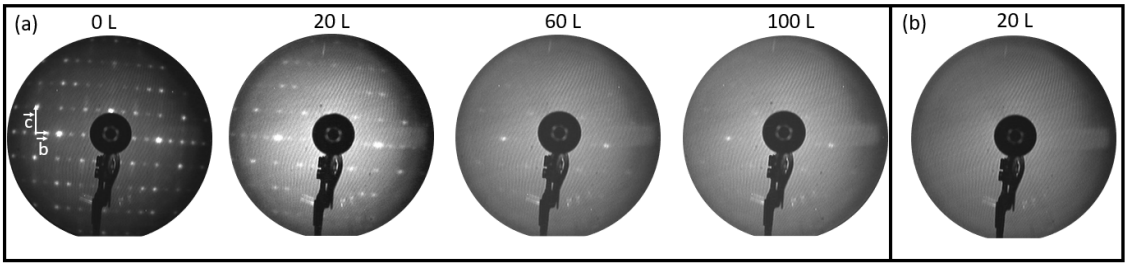

Figure 1: (a) Evolution of the LEED pattern recorded at 22 eV upon adsorption of O_2 at room temperature. (b) LEED pattern recorded at 22 eV after adsorption of 20 L of O_2 at 573 K.

60° with respect to the surface normal. The information depth by XPS is divided by a factor of two when the take-off angle measured with respect to the surface normal is increased from 0 to 60°. This is due to the fact that the information depth depends on the cosine of the take-off angle. Taking into account that Au is the principal element of the compound, it is reasonable to assume that the photoelectron mean free path is close to that in Au, that is $\lambda = 1.37$ nm considering Au 4f core level. Knowing that 63 % (resp. 95%) of the signal comes from λ (resp. 3λ), the information depth is d = $\lambda\cos\alpha$ (resp. $3\lambda\cos\alpha$) where α is the take-off angle. Therefore the information depth is reduced from 1.37 nm (resp. 4.11 nm) at 0° to 0.69 nm (resp. 2.06 nm) at 60°. Figure 2 shows the evolution of the chemical composition with photoelectron take-off angle after adsorption of 100 L of O_2 at room temperature and 573 K. At room temperature, upon increasing the surface sensitivity (from 0° to 60°), the concentration in Au decreased slightly while the Si content increased slightly. The concentration in Ho is almost constant. By comparing the concentration obtained before and after adsorption O_2 at the surface for photoelectron take-off angle of 60°, the concentration in Au decreased by 9.5% while Ho and Si concentrations increase by 2.4% and 7.1% respectively. After adsorption of 100 L of O_2 at 573 k and compared to the clean surface stoichiometry, the concentration in Au decreases by 25.4% but those of Ho and Si increase by 12.8% and 12.6% respectively. These results indicate that adsorption of O_2 induces segregation of Ho and Si at the surface. The loss of the LEED pattern discussed previously is certainly originates from Ho and Si segregation at the surface, leading to the formation of an amorphous surface oxide layer. It would appear that oxidation at room temperature limits elemental diffusion to the surface and therefore only element present within the topmost surface layer will be oxidized. For both temperature regimes, the Au core level line shape is unaffected and retains a metallic character as expected for noble metal.

Figure 3 shows the O 1s XPS core level upon adsorption of 100 L of Oxygen at room temperature and at 573 K. After oxidation at room temperature (Figure 3(a)) a single O 1s peak is observed at 531.5 eV binding energy (BE). After oxidation at 573 K, O 1s core level exhibits a shoulder on the high binding energy side and can be fitted with two components: one at low binding energy (531.3 eV) called $O(1s)_{LBE}$ and the second at higher binding energy (532.8 eV) called $O(1s)_{HBE}$. The binding energy of the O 1s core level in Ho_2O_3 trioxide is 531.1 eV [18] while it is close to 532.8 eV for SiO_x/SiO_2 [19,20]. Therefore it is likely that the shoulder appearing on the high binding energy side of the O 1s core level is due to the formation of Si-O bonds similar to silicon oxides due to the Si enrichment in the near-surface region after oxidation at 573K.

Figure 4 shows the XPS spectrum of Si and Ho taken from the 2s and 4d core levels respectively. The red spectrum in Fig. 4(a) is the spectrum obtained on the clean surface. The Ho peaks extend over a region ranging from 210 to 157 eV corresponding to the different multiplets of Ho [21]. After

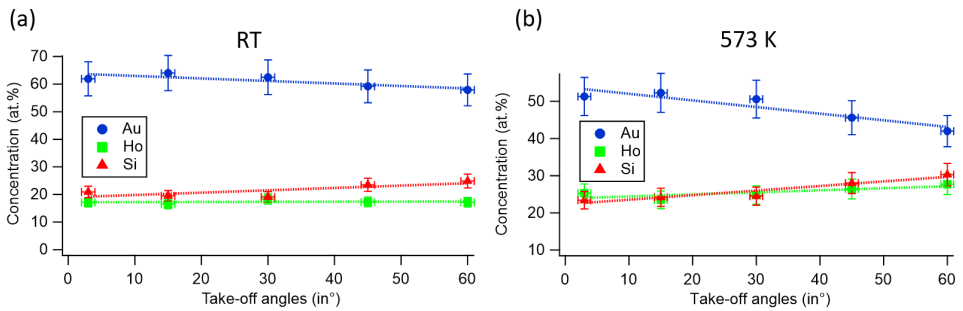

Figure 2: Variation of the elemental composition at the Au-Si-Ho(100) surface as a function of photoelectron take-off angle after adsorption of 100 L of O_2 at room temperature (RT) (a) and 573 K (b). The solid lines are just guide for the eyes. The chemical composition here is calculated from the metallic and oxidized XPS peak area of Si 2s, Ho 4d and Au 4f core levels.

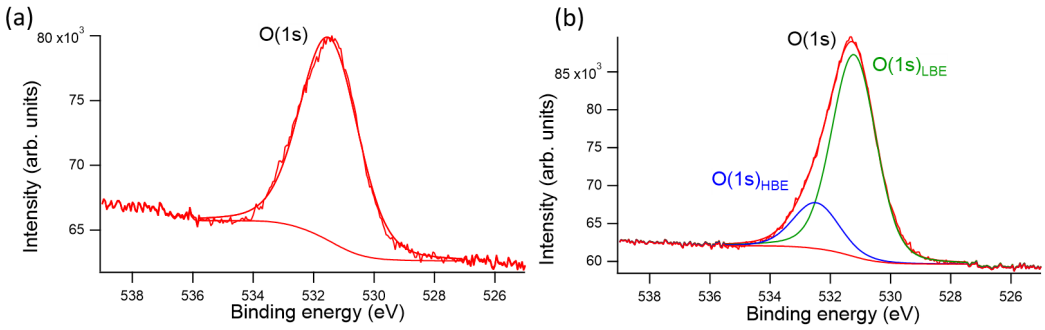

Figure 3: XPS O 1s core level after oxidation at room temperature (a) and 573 K (b).

exposing the surface to 100 L of O_2 at 573 K, the intensity of the first sharp peak at 160 eV in the Ho 4d spectrum is strongly suppressed (green curve in Fig. 4(a)) while this peak is still clearly visible (blue curve in Fig. 4(a)) after exposing the surface to 100 L of O_2 at RT. A single Si 2s peak is observed at 151.3 eV BE on the clean surface. After oxidation at 573 K, a doublet is observed (green and blue curves in Fig. 4(a)). This doublet is made up of one peak Si $2s_{LBE}$ at 151.26 eV and another one Si $2s_{HBE}$ at 153.56 eV. This latter value is close to the Si 2s BE in SiO_x (153.9 eV) [22], therefore the Si $2s_{LBE}$ and Si $2s_{HBE}$ could correspond to Si in the intermetallic compound and in SiO_2 respectively [22]. The modifications occurring in both Si 2s peak and Ho 4d peak after oxidation confirm the formation of Ho-O and Si-O bonds. The disappearance of the first sharp peak at 160 eV for Ho 4d core level and the formation of SiO_2 is much slower when oxidation takes place at room temperature whereas it is faster at 573 K (Fig 4(a)). The Au core level lineshape remains unchanged after oxidation confirming the fact that Au is almost totally inert towards oxidation.

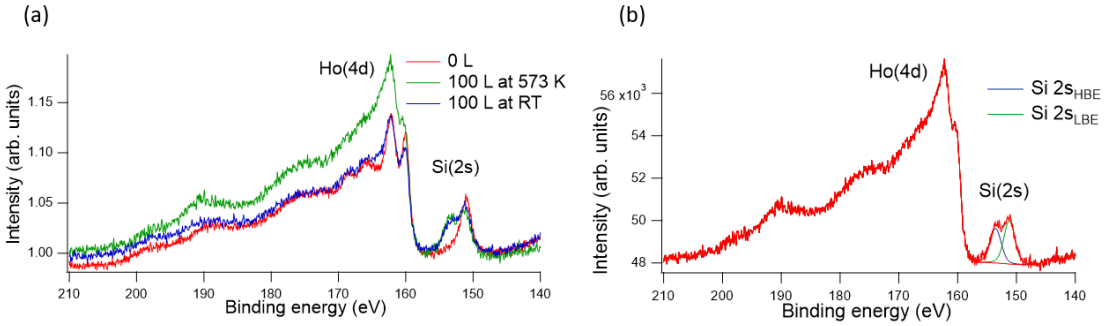

Figure 4: XPS core level of Si 1s and Ho 4d for a clean surface (0 L), after adsorption of 100 L of O_2 at room temperature (RT) and 573 K recorded at 0° (a). Fit of Si 2s after adsorption of 100 L of O_2 at 573 K (b).

4 Conclusion

The surface reactivity of Au-Si-Ho(100) surface has been studied by adsorption of O_2 using LEED and XPS. Combining these two techniques reveals that the initial stages of O_2 adsorption induces segregation of Si and Ho at the surface. This segregation at the surface creates a disorder in the structure leading to a progressive disappearance of the LEED pattern when adsorption of O_2 is done at room temperature and rapid disappearance of the LEED at 573 K. This surface oxidizes more rapidly at 573 K than at room temperature. Different oxide species are clearly formed here according to the XPS peak measured with a difficulty to fit the Ho 4d core level inherent to the presence of multiplets. It appears that Si and Ho diffusion are promoted/activated by oxidation with greater kinetics at higher temperature. Similar experiments could be carried out for different partial pressure of O_2 and for greater exposure to explore further the possibility to grow cristalline oxide thin films ontop of the Au-Si-Ho approximant.

References

[1] P. A. Thiel, "Quasicrystal Surfaces," *Annual Review of Physical Chemistry*, vol. 59, pp. 129–152, May 2008.

[2] A. Tsai and M. Yoshimura, "Highly active quasicrystalline Al-Cu-Fe catalyst for steam reforming of methanol," *Applied Catalysis A: General*, vol. 214, pp. 237–241, June 2001.

[3] V. Fournée, J. Ledieu, M. Shimoda, M. Krajčí, H.-R. Sharma, and R. McGrath, "Thin Film Growth on Quasicrystalline Surfaces," *Israel Journal of Chemistry*, vol. 51, pp. 1314–1325, Dec. 2011.

[4] H. R. Sharma, M. Shimoda, and A. P. Tsai, "Quasicrystal surfaces: structure and growth of atomic overlayers," *Advances in Physics*, vol. 56, pp. 403–464, May 2007.

[5] L. C. L. A. Jamshidi, R. J. Rodbari, L. Nascimento, E. P. Hernandez, and Celmy Maria Bezerra De Menezes Barbosa, "Formation of phase icosahedral and decagonal quasicrystalline alloys $Al_{62.2}Cu_{25.3}Fe_{12.5}/Al_{65}Ni_{15}Co_{20}$ influence on the oxidation," *Jounal of Metals Materials and*

Minerials, vol. 26, p. 1, 2016. Publisher: Metallurgy and Materials Science Research Insititute Chulalongkorn University.

[6] J.-N. Longchamp, S. Burkardt, M. Erbudak, and Y. Weisskopf, "Formation of a well ordered ultrathin aluminum oxide film on icosahedral AlPdMn quasicrystal," *Physical Review B*, vol. 76, p. 094203, Sept. 2007.

[7] D. Rouxel, M. Gil-Gavatz, P. Pigeat, and B. Weber, "Oxidation kinetics of the quasicrystalline i-AlCuFe phase compared with that of crystalline ω-AlCuFe and pure aluminum," *Journal of Non-Crystalline Solids*, vol. 351, pp. 802–809, Apr. 2005.

[8] M. Wardé, M. Herinx, J. Ledieu, L. Serkovic Loli, V. Fournée, P. Gille, S. Le Moal, and M.-G. Barthés-Labrousse, "Adsorption of O_2 and C_2H (n= 2, 4, 6) on the Al_9Co_2(001) and o-$Al_{13}Co_4$(100) complex metallic alloy surfaces," *Applied Surface Science*, vol. 357, pp. 1666–1675, Dec. 2015.

[9] M. Wardé, J. Ledieu, L. N. Serkovic Loli, M. Herinx, M.-C. de Weerd, V. Fournée, S. L. Moal, and M.-G. Barthés-Labrousse, "Growth and structure of ultrathin alumina films on the (110) surface of γ -Al_4Cu_9 complex metallic alloy," *Journal of Physics: Condensed Matter*, vol. 26, p. 485009, Dec. 2014.

[10] J. Guo, E. Abe, and A.-P. Tsai, "Stable Icosahedral Quasicrystals in the Cd–Mg–RE (RE = Rare Earth Element) Systems," *Japanese Journal of Applied Physics*, vol. 39, p. L770, Aug. 2000.

[11] H. Takakura, C. P. Gómez, A. Yamamoto, M. De Boissieu, and A. P. Tsai, "Atomic structure of the binary icosahedral Yb–Cd quasicrystal," *Nature Materials*, vol. 6, pp. 58–63, Jan. 2007.

[12] A. P. Tsai, J. Q. Guo, E. Abe, H. Takakura, and T. J. Sato, "A stable binary quasicrystal," *Nature*, vol. 408, pp. 537–538, Nov. 2000.

[13] G. Gebresenbut, T. Shiino, D. Eklöf, D. C. Joshi, F. Denoel, R. Mathieu, U. Häussermann, and C. Pay Gómez, "Atomic-Scale Tuning of Tsai-Type Clusters in RE–Au–Si Systems (RE = Gd, Tb, Ho)," *Inorganic Chemistry*, vol. 59, pp. 9152–9162, July 2020.

[14] G. H. Gebresenbut, T. Shiino, M. S. Andersson, N. Qureshi, O. Fabelo, P. Beran, D. Qvarngård, P. Henelius, A. Rydh, R. Mathieu, P. Nordblad, and C. Pay Gomez, "Effect of pseudo-Tsai cluster incorporation on the magnetic structures of ahs quasicrystal approximants," *Physical Review B*, vol. 106, p. 184413, Nov. 2022.

[15] G. H. Gebresenbut, R. Tamura, D. Eklöf, and C. P. Gómez, "Syntheses optimization, structural and thermoelectric properties of 1/1 Tsai-type quasicrystal approximants in RE–Au–SM systems (RE=Yb, Gd and SM=Si, Ge)," *Journal of Physics: Condensed Matter*, vol. 25, p. 135402, Apr. 2013.

[16] P. J. Nugent, G. Simutis, V. R. Dhanak, R. McGrath, M. Shimoda, C. Cui, A. P. Tsai, and H. R. Sharma, "Surface oxidation of the icosahedral Ag-In-Yb quasicrystal," *Physical Review B*, vol. 82, p. 014201, July 2010.

[17] S. A. Villaseca, J. Ledieu, L. N. Serkovic Loli, M.-C. de Weerd, P. Gille, V. Fournée, J.-M. Dubois, and E. Gaudry, "Structural investigation of the (001) surface of the al_9co_2 complex metallic alloy," *The Journal of Physical Chemistry C*, vol. 115, pp. 14922–14932, Aug. 2011.

[18] B. Padalia, W. Lang, P. Norris, L. Watson, and D. Fabian, "X-ray photoelectron core-level studies of the heavy rare-earth metals and their oxides," *Proceedings of the Royal Society of London. A. Mathematical and Physical Sciences*, vol. 354, pp. 269–290, May 1977.

[19] A. Cros, R. Saoudi, G. Hollinger, C. A. Hewett, and S. S. Lau, "An x-ray photoemission spectroscopy investigation of oxides grown on Au_xSi_{1-x} layers," *Journal of Applied Physics*, vol. 67, pp. 1826–1830, Feb. 1990.

[20] E. Paparazzo, "XPS and auger spectroscopy studies on mixtures of the oxides SiO_2, Al_2O_3, Fe_2O_3 and Cr_2O_3," *Journal of Electron Spectroscopy and Related Phenomena*, vol. 43, pp. 97–112, Jan. 1987.

[21] C. W. Chuang, F. M. F. de Groot, Y. F. Liao, Y. Y. Chin, K. D. Tsuei, R. Nirmala, D. Malterre, and A. Chainani, "Hard x-ray photoemission spectroscopy of GdNi and HoNi," *Physical Review B*, vol. 102, p. 165127, Oct. 2020.

[22] T. Bekkay, E. Sacher, and A. Yelon, "Surface reaction during the argon ion sputter cleaning of surface oxidized crystalline silicon (111)," *Surface Science*, vol. 217, pp. L377–L381, July 1989.